Available online at www.sciencedirect.com
SCIENCE DIRECT®
Chemical Physics Letters 368 (2003) 139–146
CHEMICAL PHYSICS LETTERS
www.elsevier.com/locate/cplett

Ab initio study of reaction mechanism of $C_2 + H_2S$

Jia-Hai Wang [a], Ke-Li Han [a,*], Guo-Zhong He [a], Zhuangjie Li [a,b,1]

[a] *State Key Laboratory of Molecular Reaction Dynamics, Dalian Institute of Chemical Physics, Chinese Academy of Sciences, Dalian 116023, China*
[b] *Department of Atmospheric Sciences, University of Illinois at Urbana-Champaign, Urbana, IL 61801, USA*

Received 31 August 2002; in final form 7 November 2002

Abstract

The reaction mechanism of $C_2 + H_2S$ has been investigated using ab initio method. On the basis of calculations using CCSD(T) in conjunction with 6-311++G(d, pd) basis set with the geometry optimized at MP2/6-311++G** level, the H-abstraction reaction on the triplet energy potential surface is an exothermic process with formation of a precomplex as an intermediate, which further dissociate to yield $HS(^2\Sigma^+) + CCH(^2\Sigma^+)$ with an energy barrier of 4.9 kcal mol^{-1}. The addition of $H_2S(^1A_1)$ to $C_2(^1\Sigma_g^+)$ on leads to a bound intermediate $H_2SCC(^1A')$ (3,3-dihydrodicarbonsulfide), which can further isomerize into $HSCCH(^1A)$ (thiohydroxyacetylene) in a one-step hydrogen migration process.

1. Introduction

Probing the history and chemical evolution of star forming regions poses a great challenge that can be partly met by putting insight into the formation of sulfur bearing molecules in extraterrestrial environments [1–9]. Besides the significant role in astrochemical processes, organosulfur molecules are also considered to be of fundamental importance in the combustion chemistry [10–12]. Succeeding an investigation on the $C(^3P_j)/H_2S$ system [13], experimental and theoretical explorations for the reaction mechanism of $C_2 + H_2S$ have been carried out recently [1], which enriched the database about the sulfur containing molecules and offered a systematic overview regarding the $C_2 + H_2S$ chemical system. In an experimental investigation $SCCH(X^2\Pi_\Omega)$ has been observed as a product from the reaction of C_2 with H_2S on singlet energy potential surface via [1],

$$C_2(^1\Sigma_g^+) + H_2S(X^1A_1) \rightarrow H_2SCC(^1A') \quad (1)$$

$$H_2SCC(^1A') \rightarrow [TS1-2]^{\neq} \rightarrow HS\text{-}CH\text{-}C(^1A') \quad (2)$$

$$HS\text{-}CH\text{-}C(^1A') \rightarrow [TS2-3]^{\neq} \rightarrow HSCCH(^1A) \quad (3)$$

$$HSCCH(^1A) \rightarrow SCCH(X^2\Pi_\Omega) + H(^2S) \quad (4)$$

* Corresponding author. Fax: +864114675584.
E-mail addresses: klhan@dicp.ac.cn (K.-L. Han), zli@atmos.uiuc.edu (Z. Li).
[1] Also corresponding author.

0009-2614/02/$ - see front matter © 2002 Elsevier Science B.V. All rights reserved.
PII: S0009-2614(02)01810-9

On the basis of calculation using CCSD(T) method with aug-cc-pVTZ basis set at the geometry optimized at B3LYP/6-311G(d, p) level, reactions (1)–(3) were predicted to be exothermic by 46.4, 41.4, and 37.5 kcal mol^{-1}, and reaction (4) was predicted to be endothermic by 75.5 kcal mol^{-1}, respectively. A key conclusion from this theoretical study is that two hydrogen migrations through the sequence of reactions (2) and (3) are required to isomerize $H_2SCC(^1A')$ into $HSCCH(^1A)$, with $HS–CH–C(^1A')$ as an intermediate species. The theoretical study also suggested that in the $C_2 + H_2S$ system there is a transition state for hydrogen abstraction on the triplet potential surface, with an energy slightly higher than the energy of separated reactants [1]. In this short Letter, we report results of our ab initio study on the reaction of C_2 with H_2S. Present study is focused on the reaction pathway of isomerization of $H_2SCC(^1A')$ leading to production of $HSCCH(^1A)$ on the singlet potential energy surface. We also examined the reaction pathway of H-abstraction reaction on the triplet potential energy surface,

$$C_2(^3\Pi_u) + H_2S(X^1A_1) \rightarrow \text{complex} \rightarrow [^3TS]^{\neq} \rightarrow HS(^2\Sigma^+) + CCH(^2\Sigma^+) \quad (5)$$

On the basis of our computational results, the rearrangement of $H_2SCC(^1A')$ into $HSCCH(^1A)$ may proceed without involvement of the $HS–CH–C(^1A')$ intermediate, and the isomerization of $H_2SCC(^1A')$ leading to formation of $HSCCH(^1A)$ appears to be a one-step process. For reaction (5) the activation energy required for the van der Waals complex to dissociate into $HS(^2\Sigma^+) + CCH(^2\Sigma^+)$ is found to be only slightly above the complex, instead of $C_2(a^3\Pi_u) + H_2S(X^1A_1)$.

2. Theoretical methods

All calculations were implemented using GAUSSIAN 98 program [14]. Reactants, products, and transition state structures involved in reactions (1)–(3) and (5) were optimized using Becke's three parameter nonlocal exchange functional theory with the nonlocal correlation functional of Lee, Yang, and Parr (B3LYP [15,16]) in conjunction with 6-311G** [17] and 6-311++G** [18] basis sets, Møller–Plesset correlation energy correction truncated at second-order (MP2) theory, and Quadratic Configuration Interaction including single and double substitutions (QCISD) theory in conjunction with 6-311++G** basis set. To obtain a better accuracy for species with very small force constants, such as $H_2SCC(^1A')$, we employed a tight option for convergence during optimizations. Single-point calculations were performed using coupled cluster theory including single, double, and triple substitutions (CCSD(T) [19,20]) in conjunction with 6-311++G(d, pd) basis set with the geometry optimized at MP2/6-311++G** level. Addition of zero point energy (ZPE) derived from frequency calculated at MP2/6-311++G** level to the single-point energy, i.e., CCSD(T)/6-311++G(d, pd)//MP2/6-311++G** + ZPE, is chosen to be the best estimated energy for the reactions in the present work.

3. Results and discussion

The optimized geometry for species involved in reactions (1)–(3) and (5) at different levels of theory is shown in Fig. 1. Total energy for each of these species is given in Table 1, and the energy level of each chemical process relative to that of the $CC(^1\Sigma_g^+) + H_2S(X^1A_1)$ reactants are summarized in Fig. 2. Energetically, our calculation predicts a triplet–singlet state separation energy of 1.5 and 1.6 kcal mol^{-1} for the C_2 molecule at CCSD(T)/6-311++G(d, pd)//MP2/6-311++G** + ZPE and CCSD(T)/6-311++G(d, pd)//QCISD/6-311++G** levels of theory, which are in good agreement with experimental value (715 cm^{-1}) 2.0 kcal mol^{-1} [21]. This suggests that calculation at CCSD(T)/6-311++G(d, pd)//MP2/6-311++G** + ZPE level of theory can provide reliable energetic results for reactions involving C_2. The calculated vibrational frequencies for the key species are provided in Table 2. The optimized reactant and product species as well as intermediate species are found to each have all positive frequencies, indicating that each of these species is a local mini-

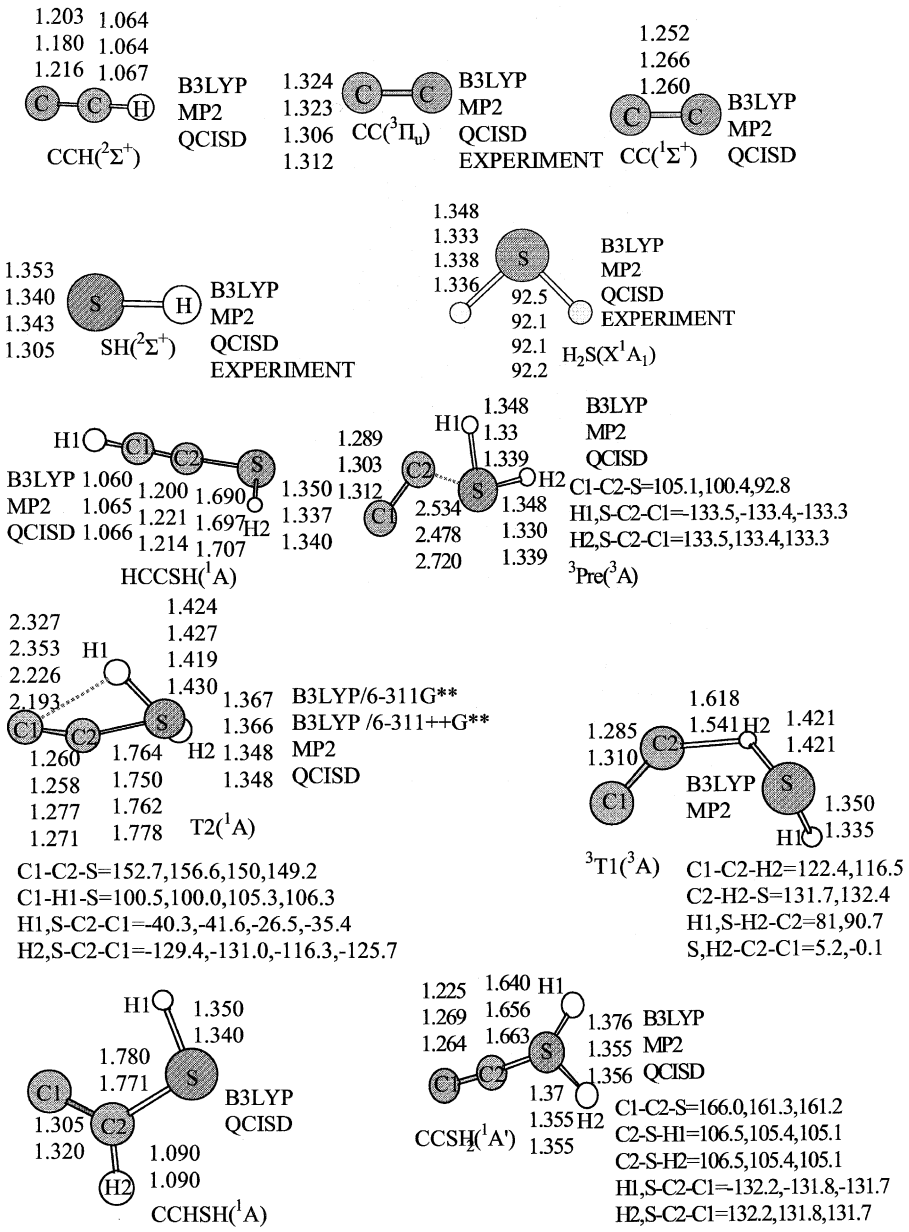

Fig. 1. Optimized geometry of reactants, products, and transition states involved in $C_2 + H_2S$. The experimental values for $^3C_2$, SH, and H_2S are from Herzberg: Molecular spectra and molecular structure, 2nd edition, volume I, and volume II.

mum on the potential energy surface. The optimized transition state configuration involved in reactions (2) and (5) possesses an imaginary frequency, indicating a saddle point on the potential energy surface for the located transition state configuration. The association of a transition state to the corresponding reactants and products was examined and confirmed by running the intrinsic reaction coordinate (IRC [22,23]) calculation to follow the reaction paths downhill in both forward and reverse directions, and the results are summarized in Figs. 3,4.

Table 1
Total energy and zero point energy (ZPE) (in Hartree) for species involved in CC + H_2S

Species[a]		ZPE	CCSD(T)[b]	CCSD(T)+ZPE
^{3}CC(M)	−75.71166	0.00375	−75.74493	−75.74118
^{3}CC(Q)	−75.73175	0.00373	−75.74492	−75.74119
CC(M)	−75.72025	0.00425	−75.74780	−75.74355
CC(Q)	−75.72287	0.00417	−75.74787	−75.74370
H_2S(M)	−398.84772	0.01569	−398.87337	−398.85768
H_2S(Q)	−398.86957	0.01545	−398.88279	−398.86734
HS(M)	−398.20610	0.00637	−398.22918	−398.22281
HS(Q)	−398.22661	0.00623	−398.23386	−398.22763
HCC(M)	−76.38049	0.01754	−76.42315	−76.40561
HCC(Q)	−76.41544	0.01467	−76.42993	−76.41526
^{3}Pre(B)	−475.37590	0.02135	−474.62534	−474.60399
^{3}Pre(M)	−474.56900	0.00222	−474.62596	−474.62374
$CCSH_2$(B)[c]	−475.43843	0.02466	−474.70178	−474.67712
$CCSH_2$(B)	−475.44364	0.02475	−474.69333	−474.66858
$CCSH_2$(M)	−474.64474	0.02564	−474.70288	−474.67724
$CCSH_2$(Q)	−474.67361	0.02538	−474.68028	−474.65490
HCCSH(B)	−475.56973	0.02696	−474.82152	−474.79456
HCCSH(M)	−474.77847	0.02656	−474.83062	−474.80406
HCCSH(Q)	−474.80377	0.02674	−474.83060	−474.80386
CCHSH(B)	−475.49817	0.02522	−474.74839	−474.72317
CCHSH(Q)	−474.73227	0.02545	−474.75747	−474.73202
^{3}T1(B)	−475.36746	0.01872	−474.61496	−474.59624
^{3}T1(M)	−474.55754	0.01953	−474.61563	−474.59610
T2(B)[c]	−475.40021	0.02155	−474.66625	−474.64470
T2(B)	−475.40572	0.02146	−474.65652	−474.63506
T2(M)	−474.60921	0.02219	−474.66670	−474.64451
T2(Q)	−474.63386	0.02192	−474.66682	−474.6449

[a] Referred to Fig. 1 for structure of each species. The superscript "3" represents the species in triplet state. M, Q, and B in parenthesis denote MP2, QCISD, and B3LYP optimization in conjunction with 6-311++G** basis set, respectively.
[b] Single-point calculation in conjunction with 6-311++G(d, pd) basis set.
[c] B3LYP optimization in conjunction with 6-311G** basis set.

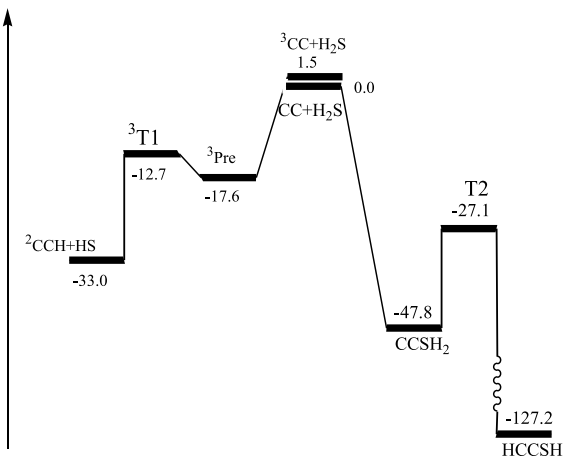

Fig. 2. Schematic energy (in kcal mol^{-1}) relative to $CC(^1\Sigma_g^+)$+ $H_2S(X^1A_1)$. The energy was computed at CCSD(T)/6-311++G(d, pd)//MP2/6-311++G** + ZPE level of theory.

Table 2
Vibrational frequency (in cm^{-1}) calculated at MP2/6-311++G** level of theory for various species involved in $C_2 + H_2S$

Species[a]	Frequency
CC	1868
TCC	1646
CCH	832, 832, 2462, 3573
H_2S	1233, 2817, 2836
SH	2797
$CCSH_2$	106, 180, 748, 920, 924, 1204, 1941, 2613, 2619
HCCSH	103, 267, 511, 680, 725, 1000, 2085, 2782, 3505
CCHSH[b]	81, 202, 607, 727, 893, 1087, 1656, 2748, 3169
^{3} T1	720*i*, 101, 137, 294, 420, 1118, 1694, 1786, 2815
T2	1198*i*, 199, 650, 891, 972, 1853, 2317, 2690
^{3}Pre	71, 149, 235, 306, 369, 1189, 1788, 2810, 2831

[a] Referred to Fig. 1 for structure of each species.
[b] Calculated at QCISD/6-311++G** level of theory.

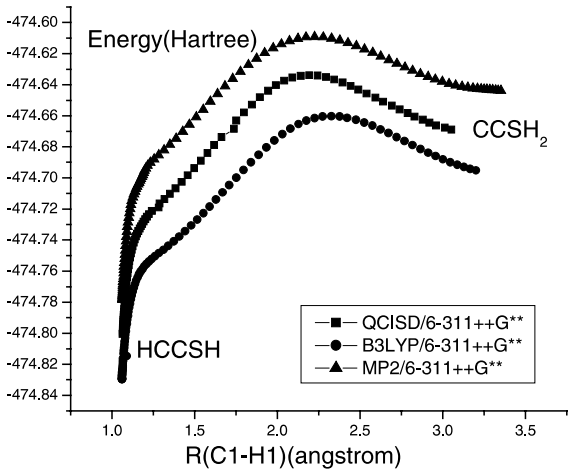

Fig. 3. Schematic potential energy profile for isomerization of $H_2SCC(^1A')$ into $HSCCH(^1A)$. 0.74 Hartree was added to the B3LYP/6-311G** energy for convenience of comparison.

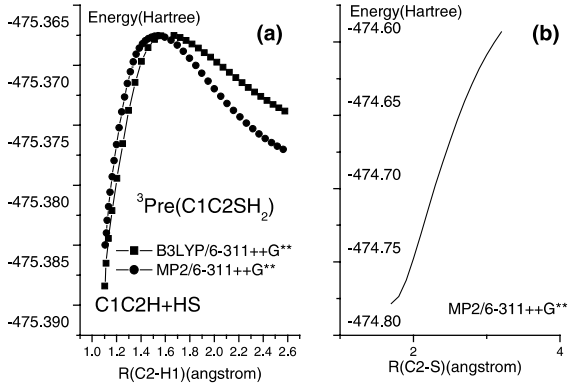

Fig. 4. (a) Schematic potential energy profile from IRC calculation staring with $^3T1$, which shows the connection of $^3T1$ to ^3Pre and $HS(^2\Sigma^+) + CCH(^2\Sigma^+)$ as reactant and products. 0.81 Hartree was added to the MP2/6-311++G** energy for convenience of comparison. (b) Schematic minimal energy profile showing the connection of $HS(^2\Sigma^+) + CCH(^2\Sigma^+)$ to $HCCSH(^1A)$.

(A) *Reaction of* $C_2(^1\Sigma_g^+)$ *with* $H_2S(X^1A_1)$. The reaction of $C_2(^1\Sigma_g^+)$ with $H_2S(X^1A_1)$ preferably forms an association intermediate $H_2SCC(^1A')$, which has been well characterized by Kaiser et al. [1]. Present study is focused on the investigation of isomerization of the $H_2SCC(^1A')$ molecule into $HSCCH(^1A)$ through H-migration. A transition state structure, namely T2 (referred to Fig. 1), was located at B3LYP/6-311G** level of theory for this process. This structure and its corresponding energy relative to $H_2SCC(^1A')$ (see Table 1) appear to be the same as that of T1-2 reported by Kaiser et al. [1] at the same level of theory. In order to find the reactant and product associated with this transition state configuration, we performed an IRC calculation at the same level of theory, and the result is shown in Fig. 3. It can be seen from Fig. 3 that H-migration transition state connects $H_2SCC(^1A')$ as the reactant and $HSCCH(^1A)$ as the product, respectively, on the singlet potential energy surface. Note that along the pathway toward the product, there is no stable intermediate between T2 and $HSCCH(^1A)$, suggesting that isomerization of $H_2SCC(^1A')$ into $HSCCH(^1A)$ through H-migration is a one-step process,

$$H_2SCC(^1A') \rightarrow [T2]^{\neq} \rightarrow HSCCH(^1A) \qquad (2')$$

This finding is in contrast to that of Kaiser et al. suggesting that the transition state is connecting to HS–CH–$C(^1A')$ as an intermediate species, which further isomerized into $HSCCH(^1A)$. To confirm this TS configuration, we also located the T2 structure and carried out the IRC calculation at both MP2/6-311++G** and QCISD/6-311++G** levels of theory. In order to obtain unambiguous species on both sides of the transition state the IRC computation was continued until the intrinsic reaction coordinates reach −7.4 and −6.5 $amu^{1/2}$ bohr on the product side, and 3.0 and 1.8 $amu^{1/2}$ bohr on the reactant side at MP2/6-311++G** and QCISD/6-311++G** level of theory, respectively. The −7.4 and −6.5 $amu^{1/2}$ bohr in the IRC runs correspond to a ca. 1.066 Å of the C1–H1 bond on the product side, and 3.0 and 1.8 $amu^{1/2}$bohr correspond to a 3.2 Å of the C1–H1 bond on the reactant side, respectively. The IRC results are also given in Fig. 3, which are consistent with that predicted at the B3LYP/6-311G** level of theory. This leads us to conclude that during the isomerization a hydrogen atom in the $H_2SCC(^1A')$ molecule bypasses the internal carbon and migrates directly from the sulfur atom to the terminal carbon, and it is this one-step, instead of two steps, of H-migration that results in the formation of $HSCCH(^1A)$. Note that the stable

CCHSH was located at both B3LYP/6-311++G** and QCISD/6-311++G** levels of theory, but not at the MP2/6-311++G** level of theory. This was also experienced in the optimization of CCHOH, a species analogous to CCHSH [24]. Nevertheless, this should not alter our conclusion based on our IRC computational results at three different levels of theory.

Besides IRC execution, we scanned, at B3LYP/6-311++G** level of theory, the minimum energy path for isomerization of $CCSH_2$ to CCHSH by fixing the C2–H1 bond (referred to Fig. 1) at several bond lengths along the pathway with other internal coordinates optimized. The optimized energy profile manifests that the reaction must overcome two energy barriers (with ca. 19 kcal mol^{-1} for the first one) to produce HS–CH–C(^{1}A). When we relaxed all structural parameters starting between the first barrier and the second barrier to optimize the system, the final product was eventually HCCSH.

(b) *Reaction of* $C_2(a^3\Pi_u)$ *with* $H_2S(X^1A_1)$. Our calculation results suggest that reaction (5) proceeds through a process leading to formation of a complex followed by the dissociation of the complex into $CCH(^2\Sigma^+)$ and $SH(^2\Sigma^+)$ products. At B3LYP/6-311G** level of theory, the C2–S bond in the complex is predicted to be 2.534 Å, indicating a weakly bond with van der Waals forces for the intermediate (see Fig. 1). The structure of the transition state predicts a 1.618 and 1.421 Å for the C2–H1 and the H1–S bond length, respectively, which is longer than the C2–H bond in $CCH(^2\Sigma^+)$ by 0.554 Å, and than the S–H bond in $SH(^2\Sigma^+)$ by 0.068 Å, respectively (see Fig. 1). The $CCH(^2\Sigma^+) + SH(^2\Sigma^+)$ system is correlated to HSCCH(^{1}A), and hence can associate to produce HSCCH(^{1}A),

$$CCH(^2\Sigma^+) + SH(^2\Sigma^+) \rightarrow HSCCH(^1A) \qquad (6)$$

It is conceivable that reaction (6) may proceed with a barrierless entrance since HSCCH(^{1}A) is a closed shell molecule. As shown in Fig. 2, the triplet $C_2(a^3\Pi_u)$ and $H_2S(X^1A_1)$ react to form a van der Waals complex with an exothermicity of 19.2 kcal mol^{-1}. Notice that this feature is distinct from the reaction of triplet C_2 with H_2O, which does not involve a complex formation [24].

At CCSD(T)/6-311++G**//MP2/6-311++G** + ZPE level of theory, an activation energy barrier of 4.8 kcal mol^{-1} is predicted for the dissociation of the complex into $CCH(^2\Sigma^+) + SH(^2\Sigma^+)$ products. We performed an IRC calculation to examine the reactant–product connection of the transition state located on the triplet potential energy surface, and the result is shown in Fig. 4. It can be seen from Fig. 4a that the transition state connect to the complex and $CCH(^2\Sigma^+) + SH(^2\Sigma^+)$ as the reactant and the products, respectively. Our computational results thus suggest that the energy of the transition state is lower than that of the triplet separate reactant by 14.4 kcal mol^{-1}, and lower than that of the singlet separate reactants by 12.8 kcal mol^{-1}, respectively (see Fig. 2). This is also in contrast to Kaiser et al.'s findings of slightly higher transition state energy than the separate reactants for the complex dissociation on the triplet potential energy surface [1]. Also on the basis of our computational results at this level of theory, the energy barrier of 4.8 kcal mol^{-1} can be readily overcome by the heat of 19.2 kcal mol^{-1} released from the complex formation process on the triplet energy surface. As a result reaction (5) would proceed rapidly to form $CCH(^2\Sigma^+) + SH(^2\Sigma^+)$, and followed by reaction (6) which show repulsive character in Fig. 4b to produce HSCCH.

Analysis of the complex molecular valence orbitals indicated that there is a weak bond between π bond of $C_2(^3\Pi_u)$ and the *n* electrons of sulfur atom, which may contribute to the large exothermicity for the complex formation process on the triplet potential surface (see Fig. 5). In fact the ∠(C1–C2–S) angle in the complex was calculated to be 105°, which reflects the orientation of the interaction between sulfur atom and carbon atom due to the interaction between π bond of $C_2(^3\Pi_u)$ and the unpaired electrons in the sulfur atom in $H_2S(X^1A_1)$.

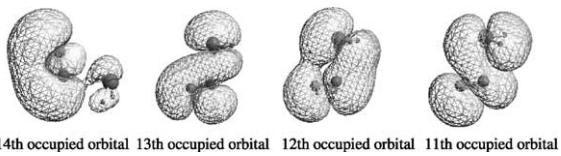

Fig. 5. The triplet state precomplex molecular valence orbitals calculated at B3LYP/6-311++G** level of theory.

The computational results from present study suggest that the H-abstraction pathway on the triplet potential energy surface leading to formation of $CCH(^2\Sigma^+) + SH(^2\Sigma^+)$ and the addition pathway on the singlet surface resulting in $HSCCH(^1A)$ for reaction of C_2 with H_2S are both exothermic processes. Due to the fact that the energy barrier is much lower than the exothermicity of these reactions, the independent reaction channels are expected to take place rapidly. Since $HSCCH(^1A)$ can be generated from reaction (6), reaction of triplet C_2 with H_2S can give rise to $HSCCH(^1A)$ through H-abstraction with intermediate $CCH(^2\Sigma^+)$ and $SH(^2\Sigma^+)$, or singlet C_2 and H_2S can lead to $HSCCH(^1A)$ through addition on the singlet potential energy surface. In this Letter, our geometry optimization is based on higher level of basis set than [1] and on careful IRC completion. Obviously T2 transition structures with B3LYP/6-311G** is similar to the TS1-2 transition structure in [1]. The IRC (Fig. 3) based on the transition show conclusive evidence that T2 connect with $CCSH_2$ and HCCSH. So, maybe the difference is caused by different basis set and the extent of competence of IRC.

4. Conclusion

We have used ab initio theory to investigate the reaction of dicarbon molecule with hydrogen sulfide molecules. At CCSD(T)/6-311++G(d, pd)//MP2/6-311++G** + ZPE level of theory, our computational results suggest that the reaction of C_2 with H_2S can take place on both triplet and singlet surfaces with large exothermicity. Results from present study are consistent with Kaiser et al. [1] in that the interaction of triplet C_2 with H_2S results in a van der Waals complex followed by its dissociation into $HS + C_2H$, and that the addition of singlet C_2 to H_2S leads to H_2SCC followed by migration of hydrogen atom from sulfur atom to the terminal carbon to form HSCCH. However, the present study found that the energy barrier of 4.8 kcal mol^{-1} associated with the dissociation of the complex into $HS + C_2H$ on the triplet potential energy surface is substantially lower, instead of slightly higher, than the energy of separated reactants as suggested by Kaiser et al. [1]. The present study also found that the isomerization of $H_2SCC(^1A')$ into $HSCCH(^1A)$ is a one-step, instead of two-step, hydrogen migration process as suggested by Kaiser et al. [1]. Finally, results from present study suggest that two independent reactions can produce $HSCCH(^1A)$, triplet C_2 and H_2S can lead to $HSCCH(^1A)$ by combination of $CCH(^2\Sigma^+)$ and $SH(^2\Sigma^+)$; singlet C_2 and H_2S can lead to $HSCCH(^1A)$ by addition of H_2S to singlet C_2 followed by reaction (2). Since $HSCCH(^1A)$ is an important source of the HSCC radical, it is likely that two independent reactions of C_2 with H_2S on both triplet and singlet could separately lead to the formation of the HSCC radical.

Acknowledgements

Thanks are expressed to The National Research Foundation of financial support.

References

[1] R.I. Kaiser, M. Yamada, Y. Osamura, J. Phys. Chem. 106 (2002) 4825.
[2] R.I. Kaiser, Chem. Rev. 102 (2002) 1309.
[3] D.J. Hollenbach, H.A. Thronson, Interstellar Processes, Reidel, Dordrecht, 1989.
[4] http:/www.cv.nrao.edu/~awootten/allmols.html.
[5] J. Chernicharo et al., AA 181 (1987) L9.
[6] S. Saito et al., ApJ 317 (1987) L115.
[7] T.J. Millar, E. Herbst, AA 231 (1990) 466.
[8] S. Petrie, MNRAS 281 (1996) 666.
[9] T. Velusamy, T.B.H. Kuiper, W.D. Langer, ApJ 451 (1995) L75.
[10] A.J. Markwich, T.J. Millar, S.B. Charnley, ApJ 535 (2000) 256.
[11] J.M. Jones et al., Carbon 33 (1995) 833.
[12] K. Schofield, Comb. Flame 124 (2001) 137.
[13] N. Galland et al., J. Phys. Chem. 105 (2001) 9893.
[14] M.J. Frisch et al., GAUSSIAN 98, revision A.9, Gaussian Inc., Pittsburgh, PA, 1998.
[15] A.D. Becke, J. Chem. Phys. 97 (1992) 9173.
[16] C. Lee, W. Yang, R.G. Parr, Phys. Rev. 37 (1988) 785.
[17] R. Krishnan, M. Frisch, J.A. Pople, J. Chem. Phys. 72 (1988) 4244.
[18] M.J. Frisch, J.A. Pople, J.S. Binkley, J. Chem. Phys. 80 (1984) 3265.
[19] G.D. Purvis, R.J. Bartlett, J. Chem. Phys. 76 (1982) 1910.

[20] K. Raghavachari, G.W. Trucks, J.A. Pople, M. Head-Gordon, Chem. Phys. Lett. 157 (1989) 479.
[21] H. Reisler, M. Mangir, C.J. Witting, J. Chem. Phys. 71 (1979) 2109.
[22] C. Gonzalez, H.B. Schlegel, J. Chem. Phys. 90 (1989) 2154.
[23] C. Gonzalez, H.B. Schlegel, J. Phys. Chem. 94 (1990) 5523.
[24] J.H. Wang, K.L. Han, G.Z. He, Z.J. Li. (submitted).